



Overview of simulations conducted by TSVV-10 on Marconi's (CPU and GPU)

A. Mishchenko on behalf of TSVV10

This work was supported in part by the Swiss National Science Foundation. Simulations presented in this work were performed on the MARCONI FUSION HPC system at CINECA. We acknowledge PRACE for awarding us access to Marconi100 at CINECA, Italy. We acknowledge PRACE for awarding us access to Joliot-Curie at GENCI@CEA, France.

MAX-PLANCK-INSTITUT
FÜR PLASMAPHYSIK

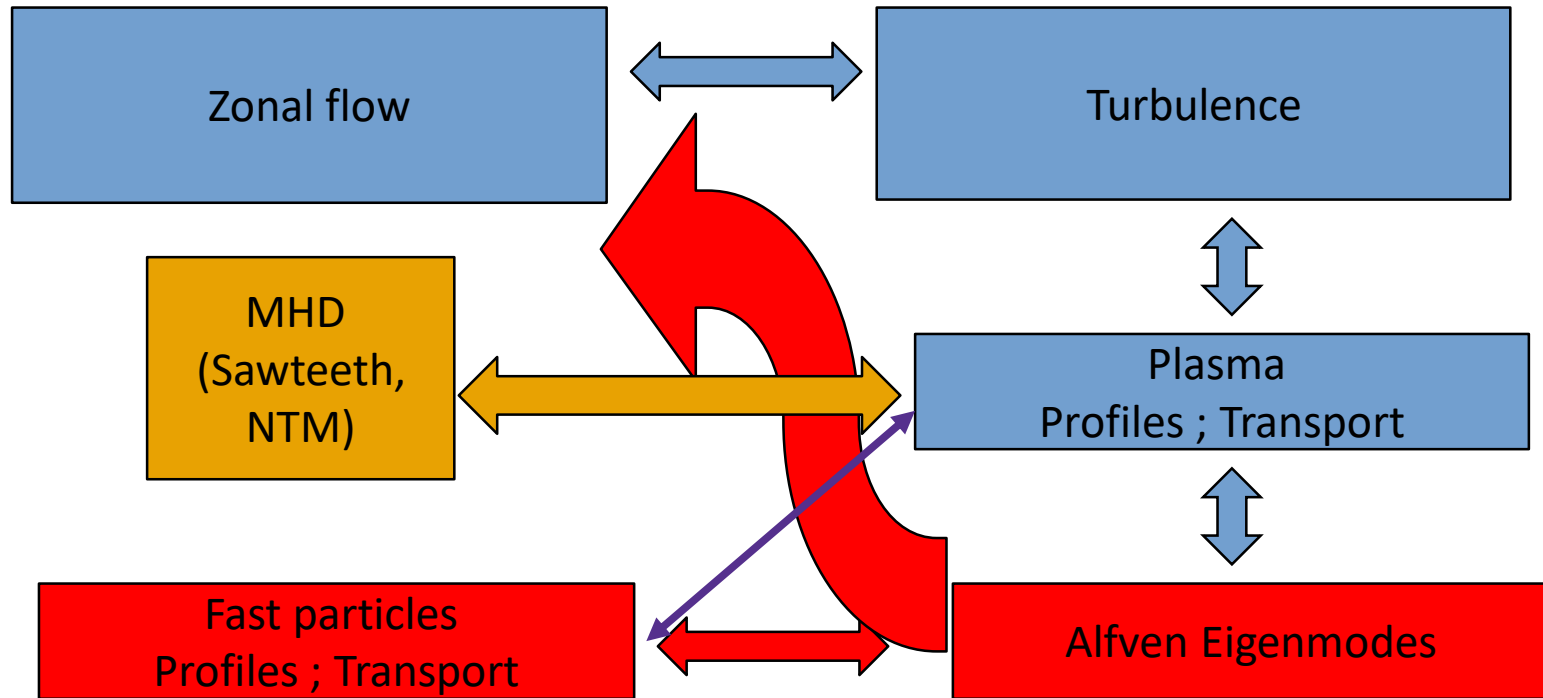


This work has been carried out within the framework of the EUROfusion Consortium, funded by the European Union via the Euratom Research and Training Programme (Grant Agreement No 101052200 — EUROfusion). Views and opinions expressed are however those of the author(s) only and do not necessarily reflect those of the European Union or the European Commission. Neither the European Union nor the European Commission can be held responsible for them.

System couplings in burning plasmas



- Energetic Particles (EP) are abundant in burning plasmas
- “Meso-scale” EP dynamics introduces couplings across scales





- Burning plasmas will have high beta and include energetic particles
- Presence of energetic particles creates complex coupled system
- Single framework including all parts consistently is needed
- Many parts of the problem are kinetic and global
- Many connections between the parts are kinetic and global
- Global gyrokinetic theory is a minimal inclusive description
- Global gyrokinetics requires intensive computation (exa-scale)

Energetic particle orbits, global Alfvénic and MHD modes, shear Alfvén continuum, avalanches, profile corrugations, phase-space structures (holes/clumps), reconnection/turbulence, Alfvén Eigenmodes-zonal flows-turbulence, ...





The equations include the gyrokinetic Vlasov equation:

$$\frac{\partial f_{1s}}{\partial t} + \dot{\mathbf{R}} \cdot \frac{\partial f_{1s}}{\partial \mathbf{R}} + \dot{v}_{\parallel} \frac{\partial f_{1s}}{\partial v_{\parallel}} = - \dot{\mathbf{R}}^{(1)} \cdot \frac{\partial F_{0s}}{\partial \mathbf{R}} - \dot{v}_{\parallel}^{(1)} \frac{\partial F_{0s}}{\partial v_{\parallel}}, \quad (1)$$

the equations for the gyro-center orbits:

$$\dot{\mathbf{R}} = \dot{\mathbf{R}}^{(0)} + \dot{\mathbf{R}}^{(1)}, \quad \dot{v}_{\parallel} = \dot{v}_{\parallel}^{(0)} + \dot{v}_{\parallel}^{(1)} \quad (2)$$

$$\dot{\mathbf{R}}^{(0)} = v_{\parallel} \mathbf{b}_0^* + \frac{1}{qB_{\parallel}^*} \mathbf{b} \times \mu \nabla B, \quad \dot{v}_{\parallel}^{(0)} = - \frac{\mu}{m} \mathbf{b}_0^* \cdot \nabla B \quad (3)$$

$$\dot{\mathbf{R}}^{(1)} = \frac{\mathbf{b}}{B_{\parallel}^*} \times \nabla \langle \phi - v_{\parallel} A_{\parallel}^{(s)} - v_{\parallel} A_{\parallel}^{(h)} \rangle - \frac{q}{m} \langle A_{\parallel}^{(h)} \rangle \mathbf{b}_0^* \quad (4)$$

$$\dot{v}_{\parallel}^{(1)} = - \frac{q}{m} \left[\mathbf{b}^* \cdot \nabla \langle \phi - v_{\parallel} A_{\parallel}^{(h)} \rangle + \frac{\partial}{\partial t} \langle A_{\parallel}^{(s)} \rangle \right] - \frac{\mu}{m} \frac{\mathbf{b} \times \nabla B}{B_{\parallel}^*} \cdot \nabla \langle A_{\parallel}^{(s)} \rangle \quad (5)$$

$$\mathbf{b}^* = \mathbf{b}_0^* + \frac{\nabla \langle A_{\parallel}^{(s)} \rangle \times \mathbf{b}}{B_{\parallel}^*}, \quad \mathbf{b}_0^* = \mathbf{b} + \frac{mv_{\parallel}}{qB_{\parallel}^*} \nabla \times \mathbf{b} \quad (6)$$

$$B_{\parallel}^* = B + \frac{mv_{\parallel}}{q} \mathbf{b} \cdot \nabla \times \mathbf{b}, \quad (7)$$

Field equations:

$$- \nabla \cdot \left(\frac{n_0}{B\omega_{ci}} \nabla_{\perp} \phi \right) = \bar{n}_{1i} - \bar{n}_{1e}$$

$$\frac{\partial}{\partial t} A_{\parallel}^{(s)} + \mathbf{b} \cdot \nabla \phi = 0,$$

$$\sum_{s=i,e} \frac{\beta_s}{\rho_s^2} A_{\parallel}^{(h)} - \nabla_{\perp}^2 A_{\parallel}^{(h)} = \mu_0 \sum_{s=i,e} \bar{j}_{\parallel 1s} + \nabla_{\perp}^2 A_{\parallel}^{(s)}$$





- “Klimontovich” representation for perturbed distribution function:

$$\delta f_s(\mathbf{R}, v_{\parallel}, \mu, t) = \sum_{\nu=1}^{N_p} w_{s\nu}(t) \delta(\mathbf{R} - \mathbf{R}_{\nu}) \delta(v_{\parallel} - v_{\nu\parallel}) \delta(\mu - \mu_{\nu}) ,$$

- Maxwellian distribution for all species:

$$F_{0s} = n_0 \left(\frac{m}{2\pi T_s} \right)^{3/2} \exp \left[- \frac{m_s v_{\parallel}^2}{2T_s} \right] \exp \left[- \frac{m_s v_{\perp}^2}{2T_s} \right]$$

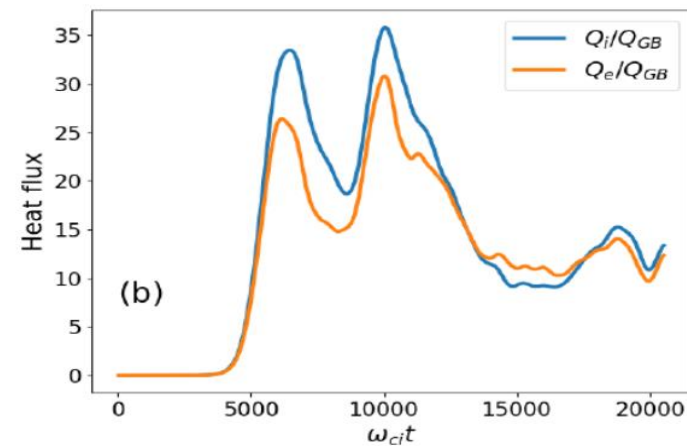
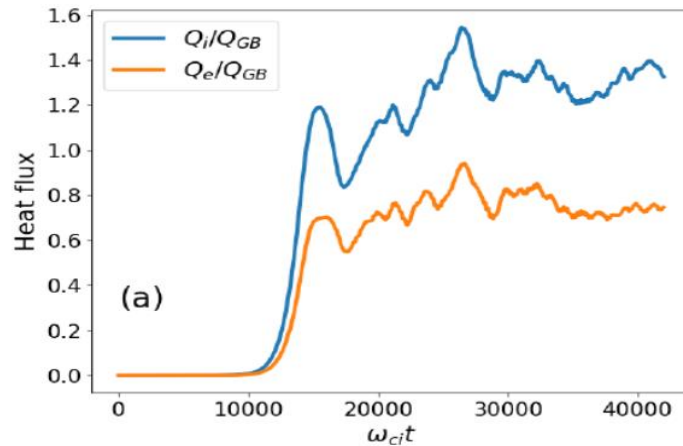
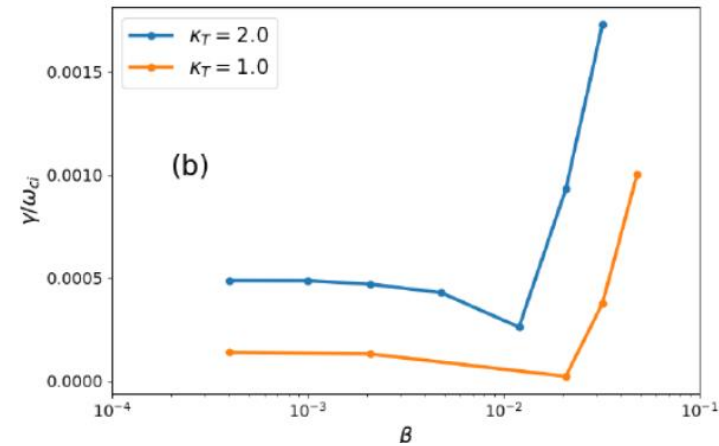
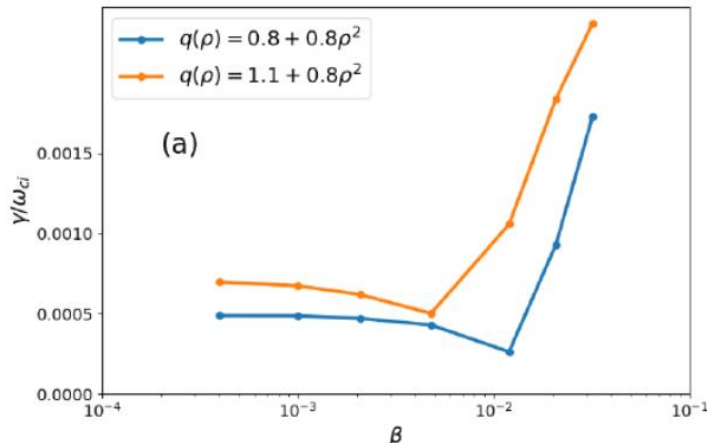
- Finite-element discretization for fields:

$$\phi(\mathbf{x}) = \sum_{l=1}^{N_s} \phi_l(t) \Lambda_l(\mathbf{x}) , \quad A_{\parallel}(\mathbf{x}) = \sum_{l=1}^{N_s} a_l(t) \Lambda_l(\mathbf{x}) ,$$

- Larmor structure for GPU-enabling in ORB5; openacc
- GPU-enabling of EUTERPE: separate routines for different particle species;
- openacc, now transitioning to openmp 5.x (wider support, more architectures)
- Replacing „globals“ (global data) with Fortran abstract types
- Gradual transition of the code base (EUTERPE) to C++
- Following general trends in HPC (abstract types, C++, accelerated hardware)
- Better access to accelerator frameworks (such as Kokkos)



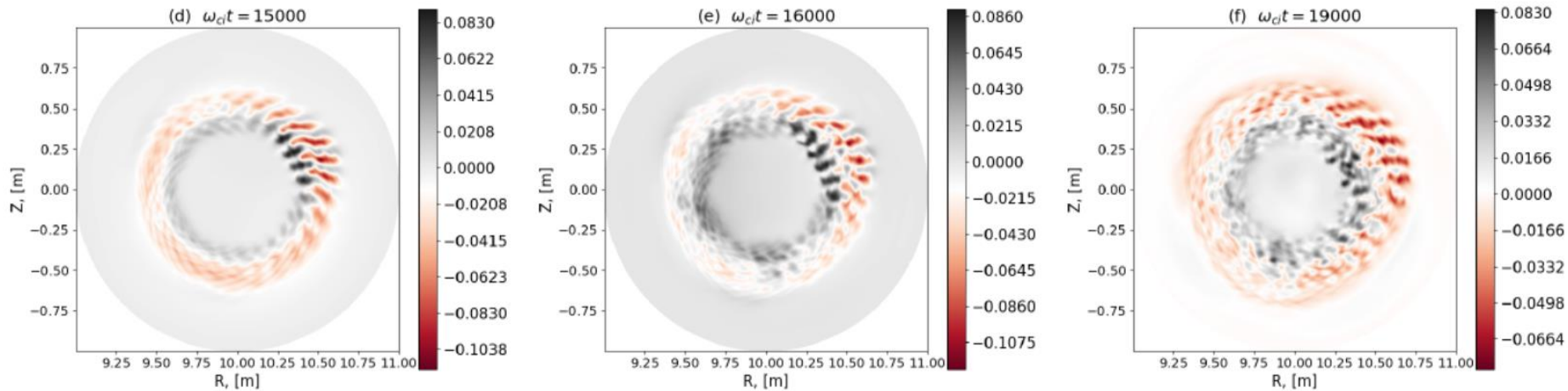
Electromagnetic turbulence in tokamak plasmas



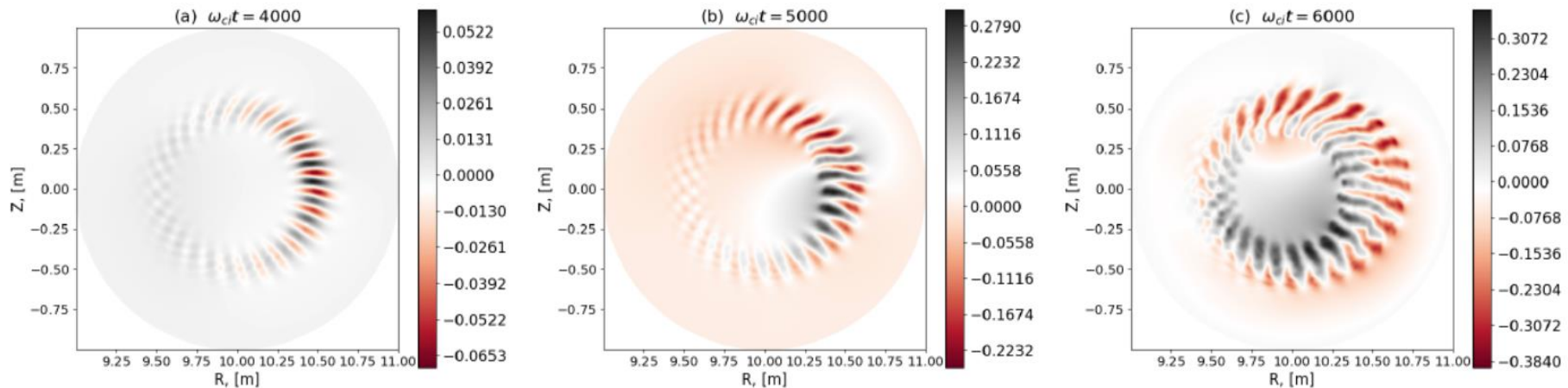
(1) Linear growth rate in circular-shaped tokamak for different safety factor profiles and temperature gradients showing electromagnetic ITG-to-KBM transition (ORB5 simulations on Marconi100, CINECA). Heat flux in the gyro-Bohm units for (a) $\beta = 0.1\%$ (electromagnetic ITG) and (b) $\beta = 2.08\%$ (KBM regime). The heat flux is considerably larger in KBM regime.

No “electromagnetic run-away” in global tokamak simulations.

EM turbulence in circular cross-section tokamak

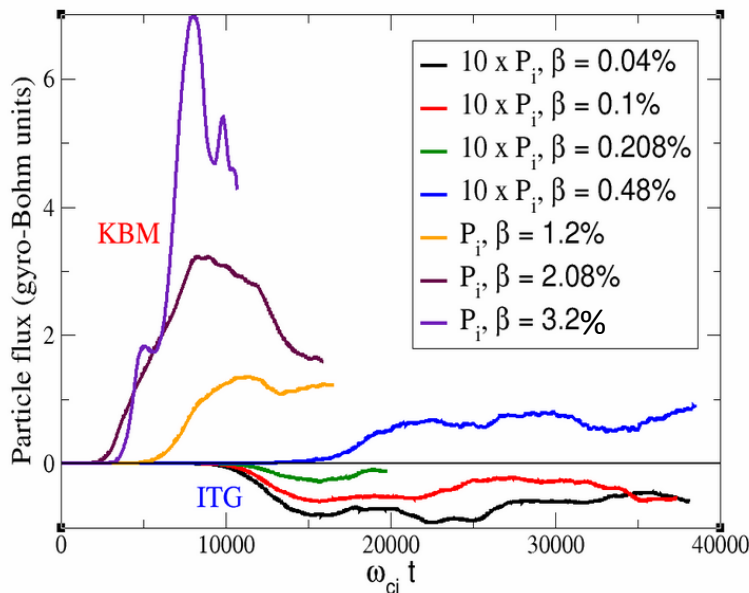
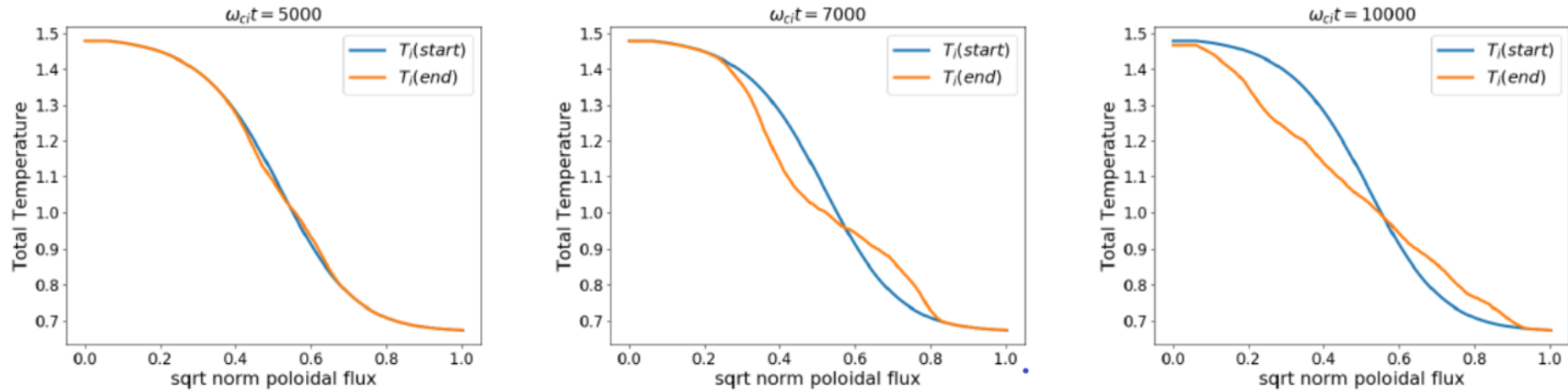


“Eddy shearing” in EM-ITG regime



Finger-like structures expelled out of “drive region” in KBM regime

EM turbulence in circular cross-section tokamak

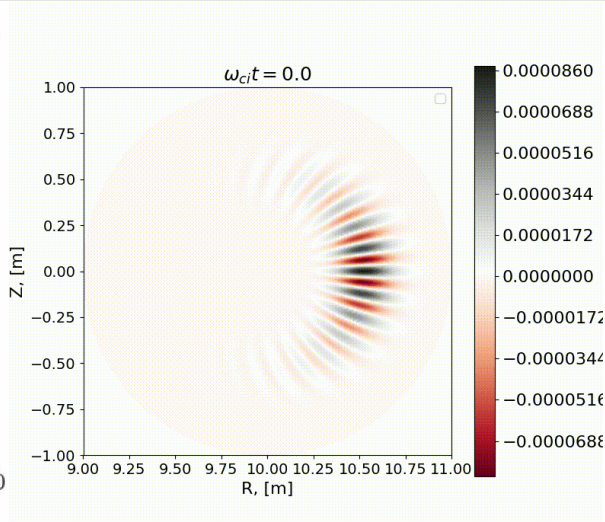
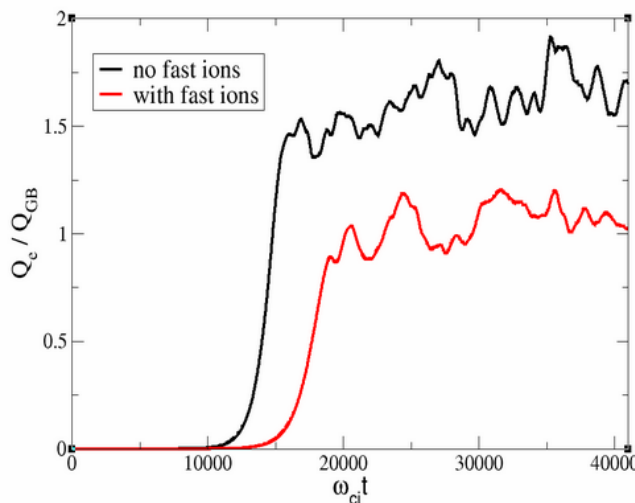
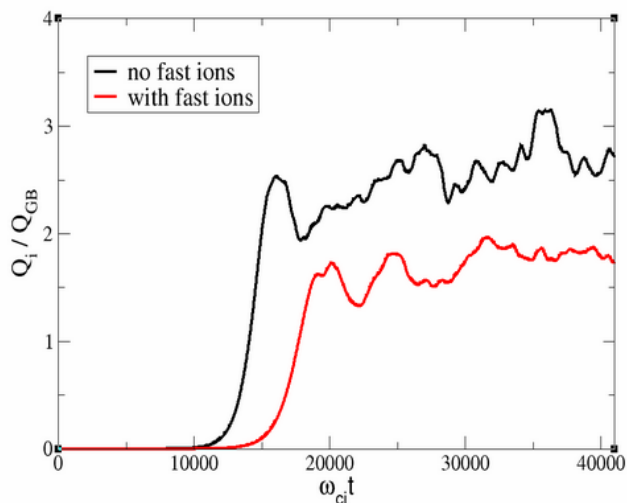


Evolution of KBM finger-like structures is accompanied by strong avalanche-like relaxation of temperature profile

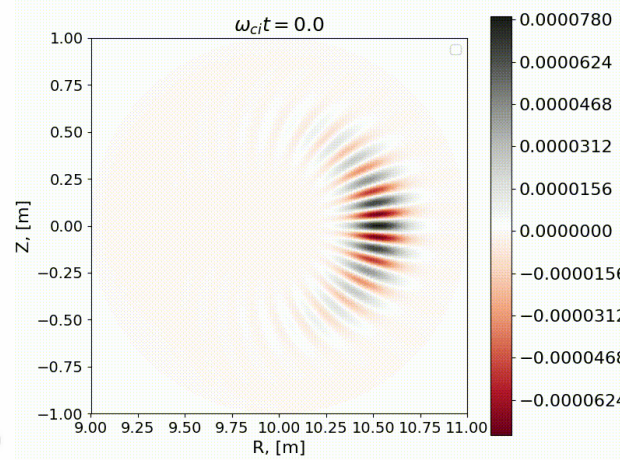
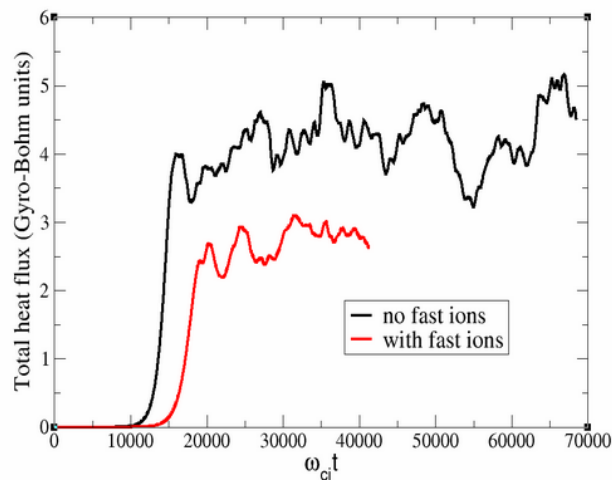
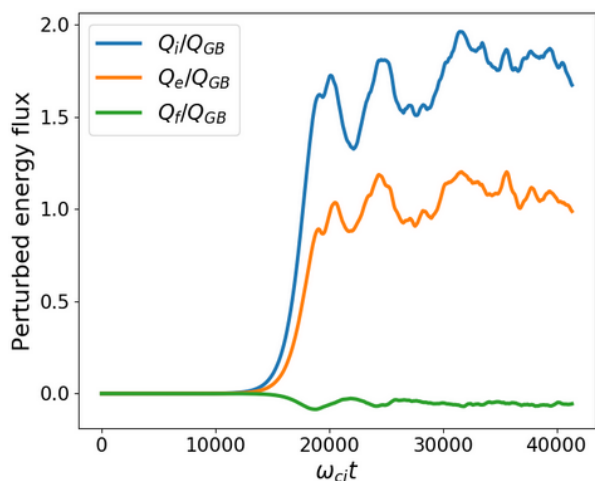
Particle flux is inward for ITGs and outward for KBMs

Density peaking in the ITG regime

Fast ion stabilization of EM turbulence

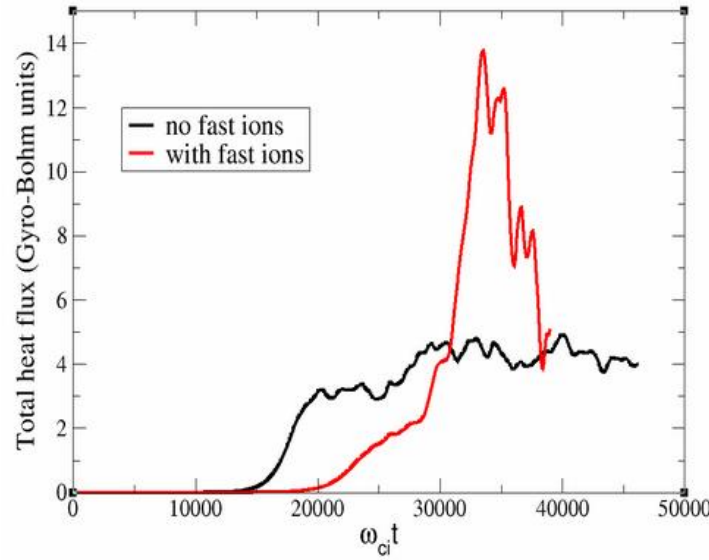
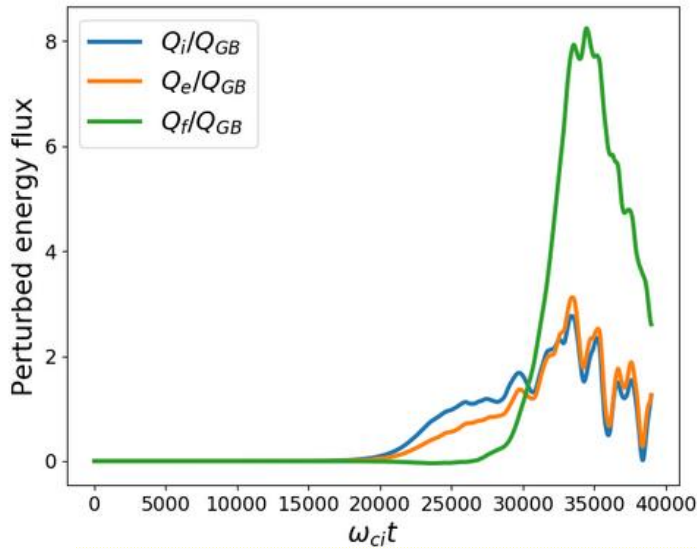


One observes a clear reduction in the heat flux for both the bulk ions and the electrons!



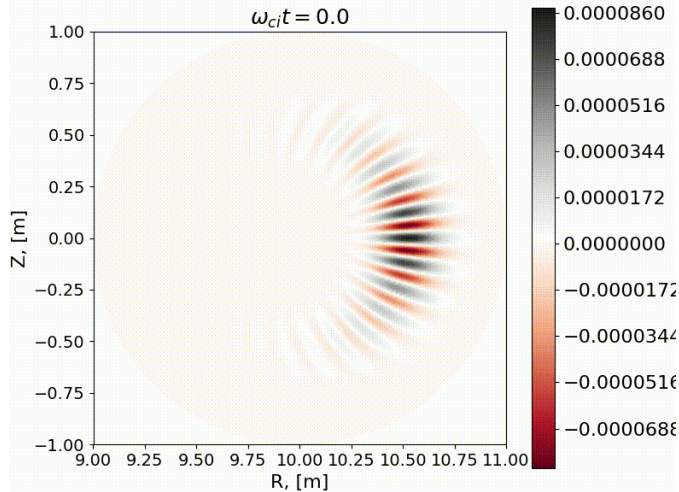
Fast ion do not transport much of energy. Total heat flux reduced by the fast ions! $\beta_e = 0.1\%$

Fast ion stabilization of EM turbulence

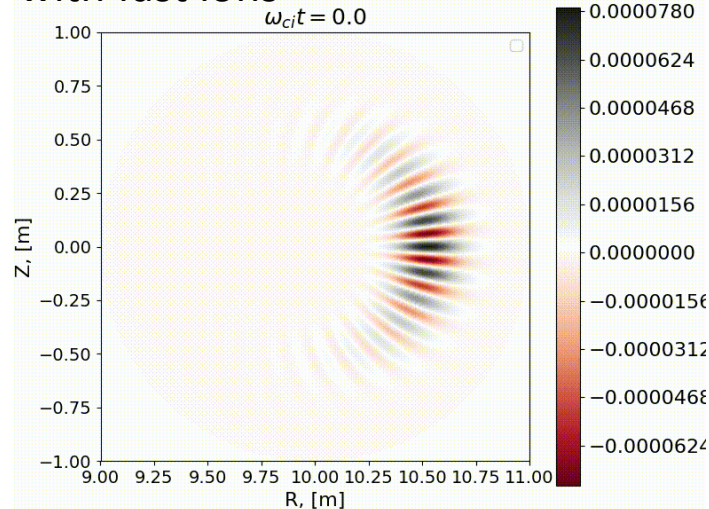


For $\beta_e = 0.24\%$, the dynamics is different. Fast ion heat flux is substantial. Total heat flux is not reduced!

no fast ions

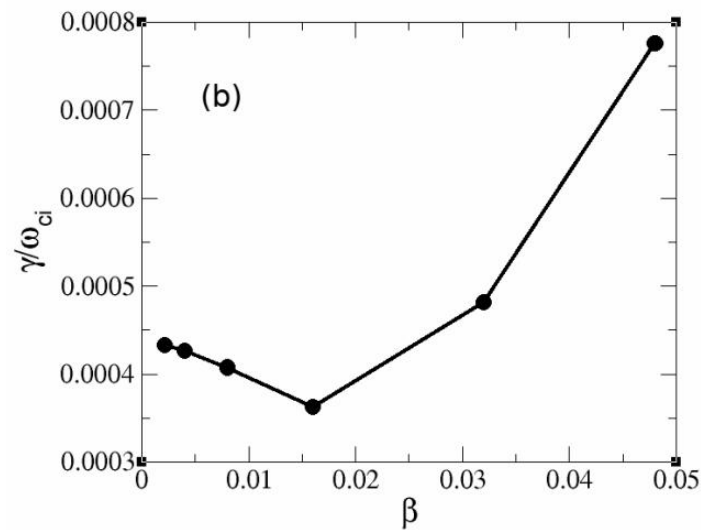
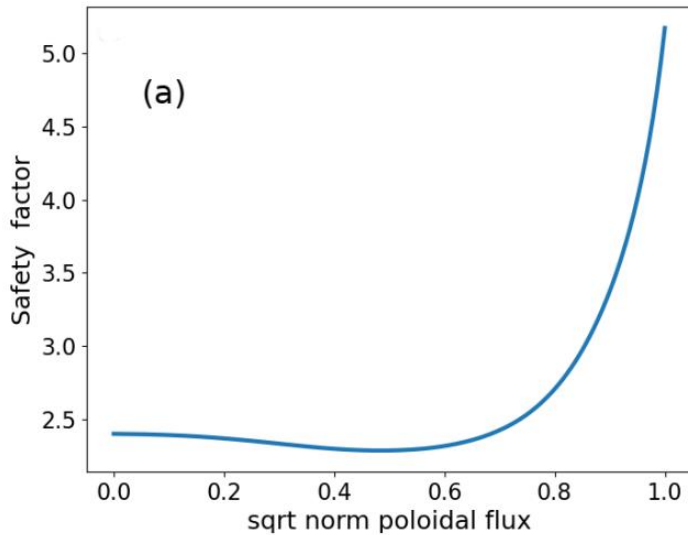


with fast ions

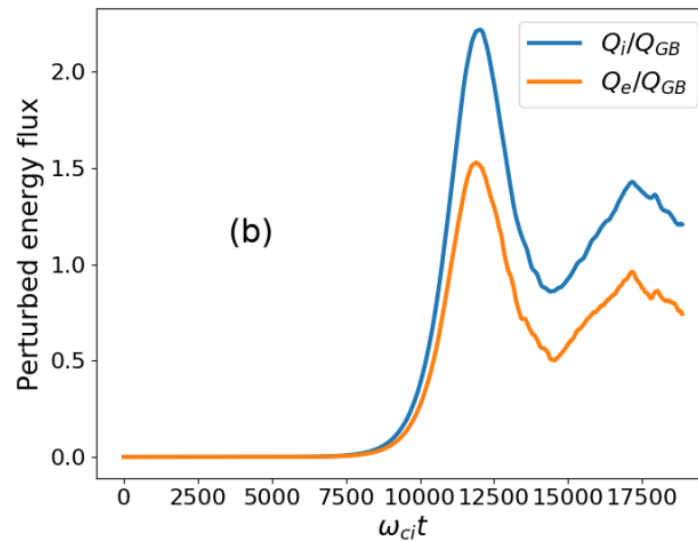
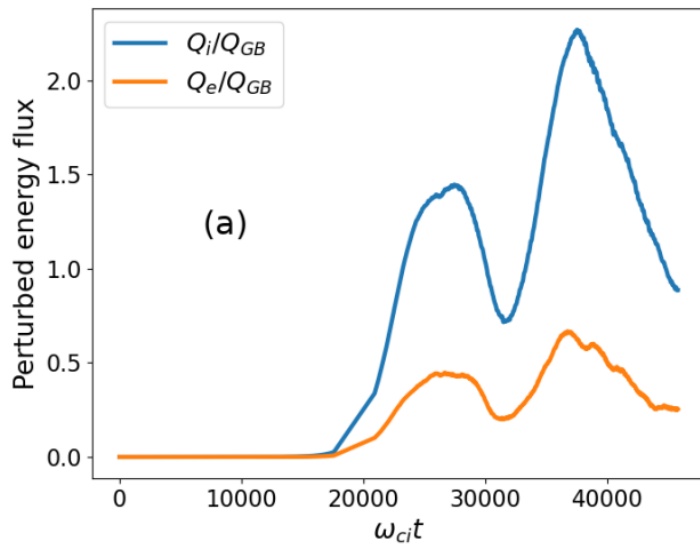


Global Alfvénic mode (a BAE?) develops driving fast ion energy flux. Work in progress!

EM Turbulence simulations in ASDEX-Upgrade

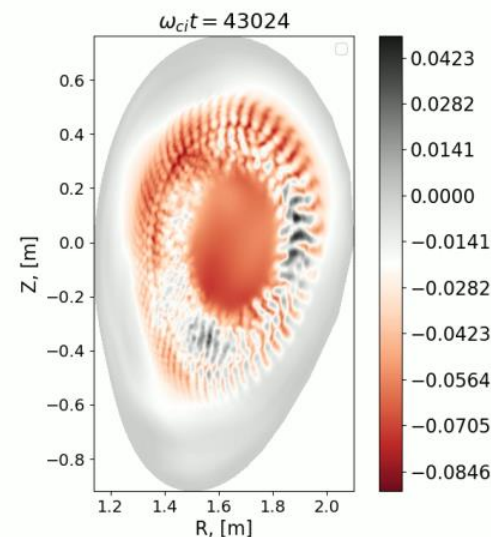
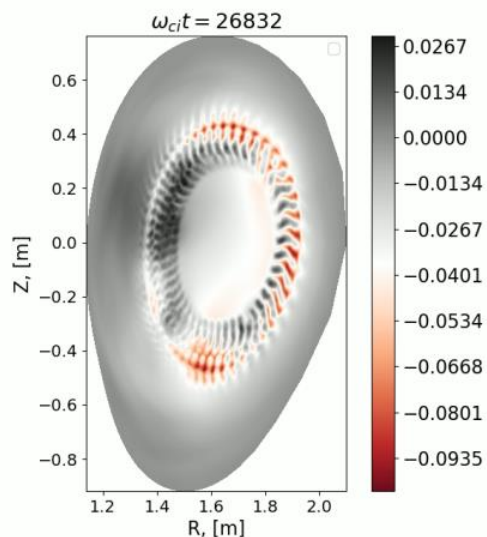
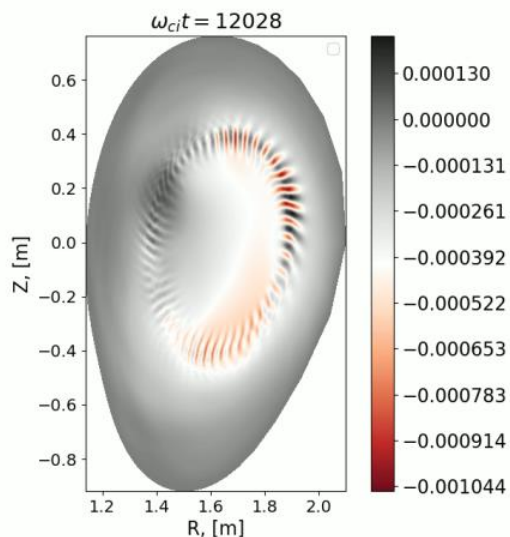


NLED-AUG case

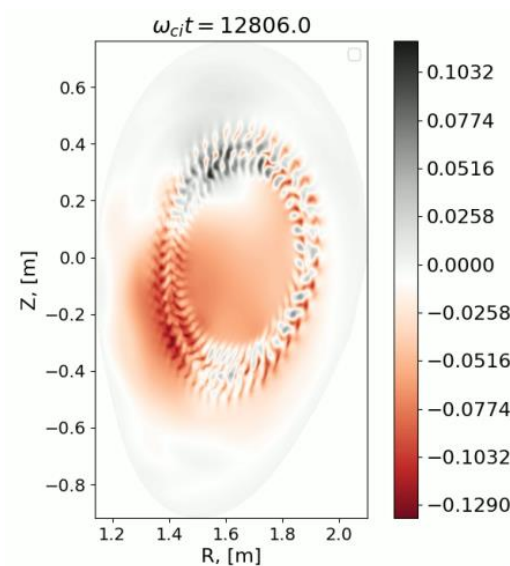
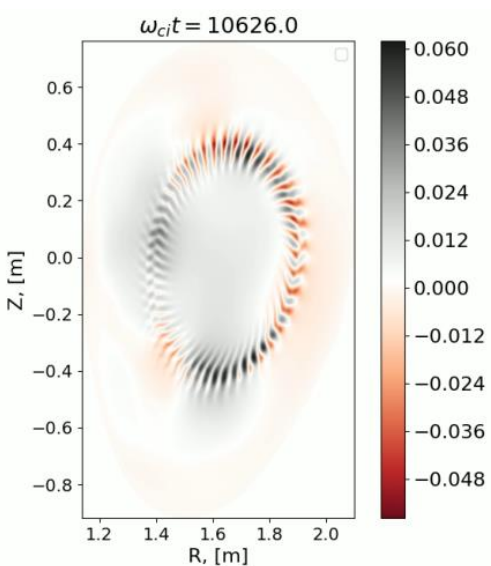
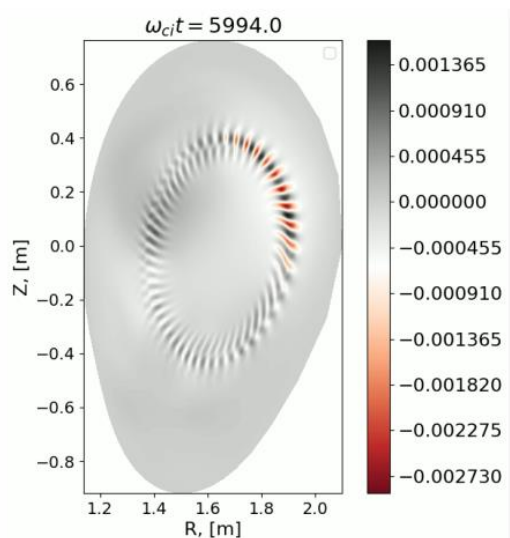


Oscillating fluxes may be caused by radial motion of max. gradient

Real-space mode structure in ASDEX-Upgrade



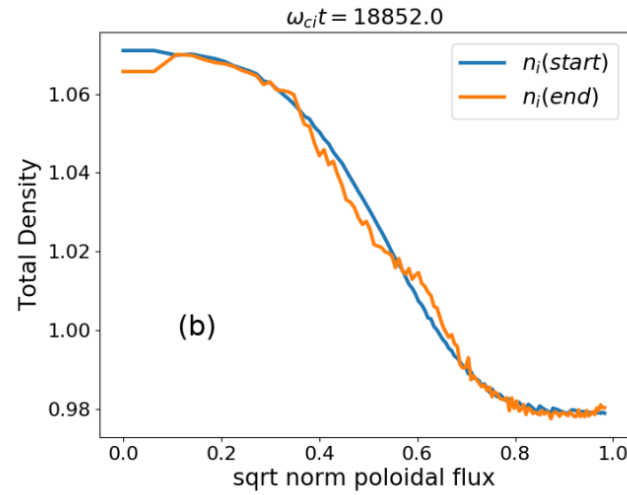
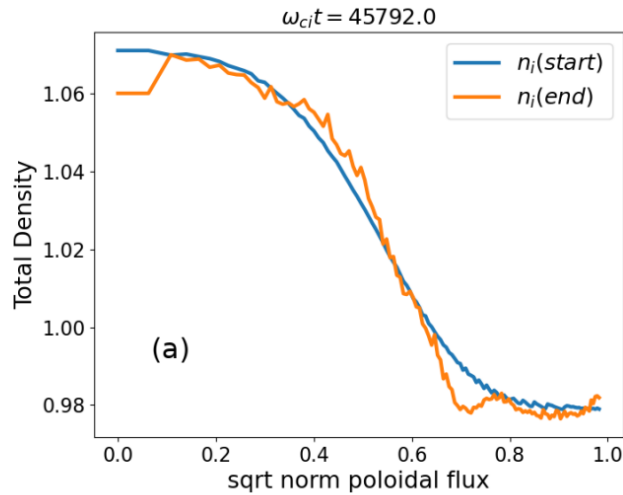
EM ITG, $\beta = 0.4\%$



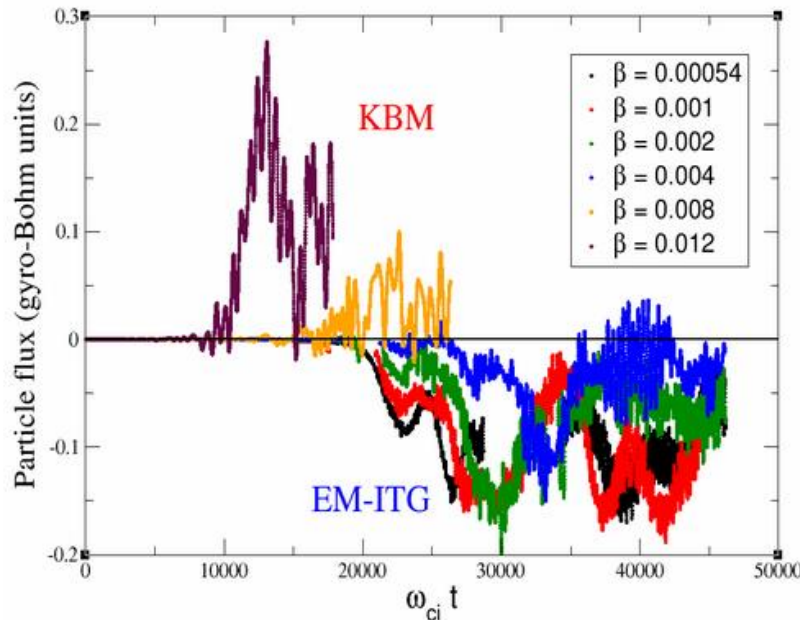
KBM, $\beta = 4.8\%$



EM particle flux in ASDEX-Upgrade

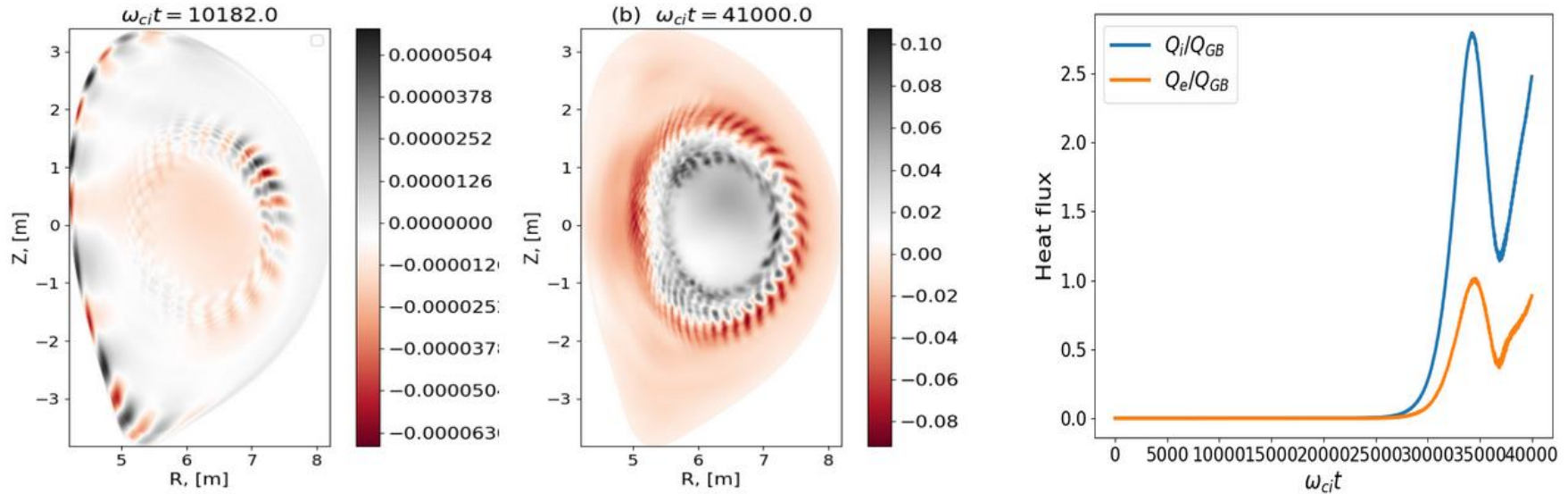


- (a) $\beta = 0.4\%$ (EM-ITG)
- (b) $\beta = 4.8\%$ (KBM)



- Inward particle flux is observed for ITGS
- For KBMs, particle flux changes sign (outward)
- Density peaking in ITG regime

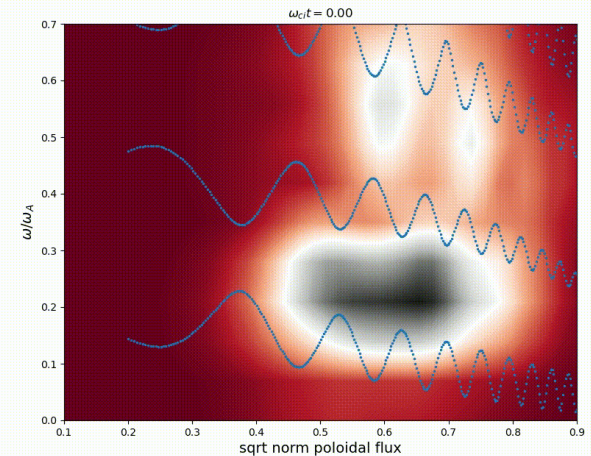
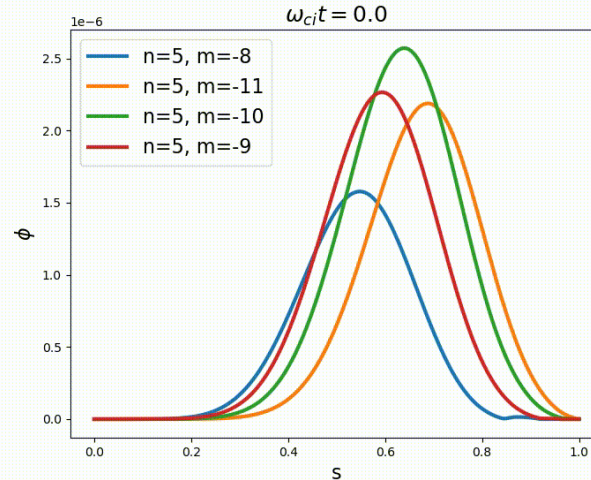
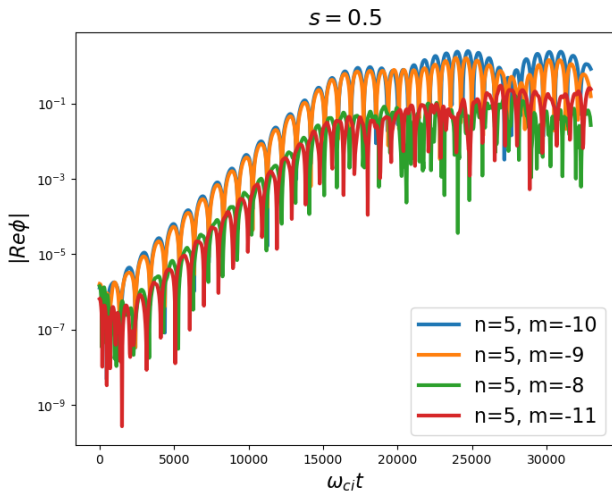
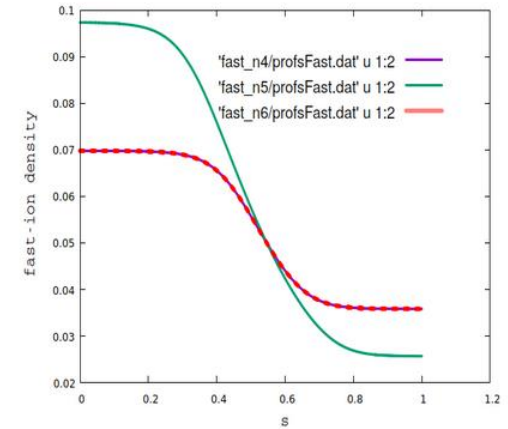
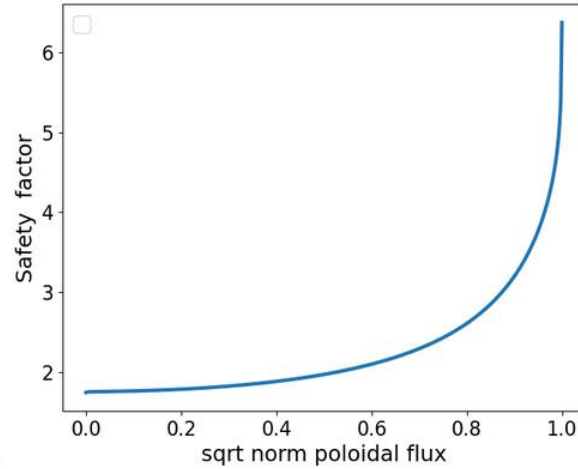
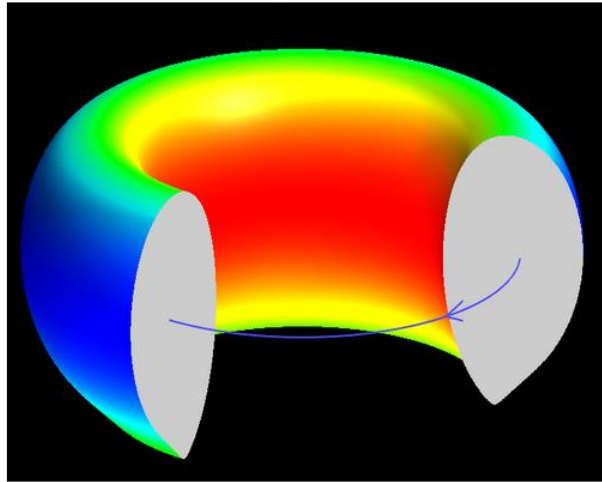
EM simulations in ITER geometry



Simulation crashes for radial resolution 288 grid points (left) but works fine for 512 points (middle and right)

Here again: oscillations in the radial flux
Consequence of non-local profile relaxation?

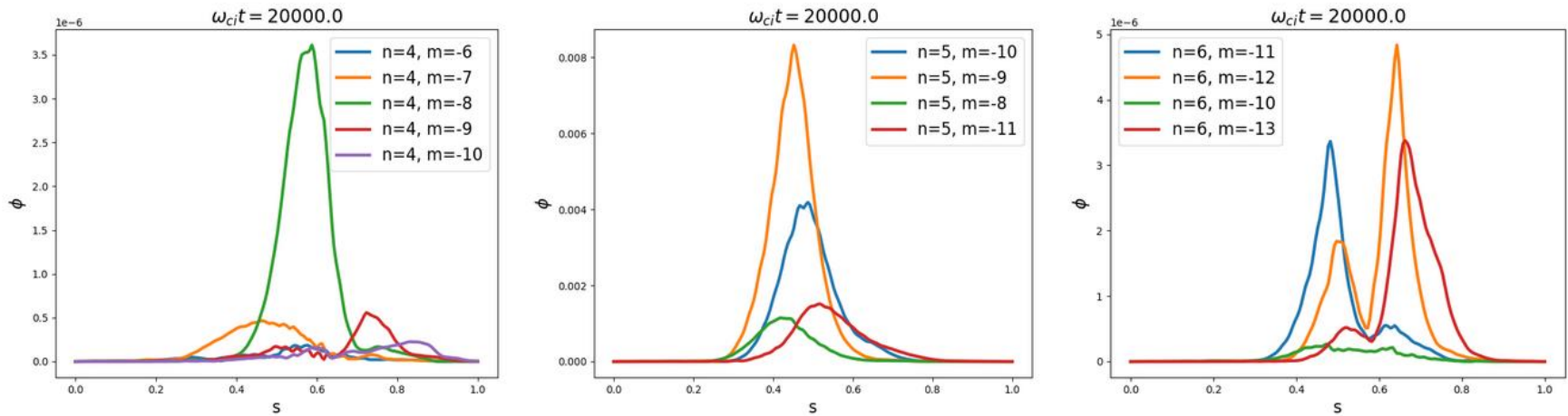
EM simulations in JET geometry



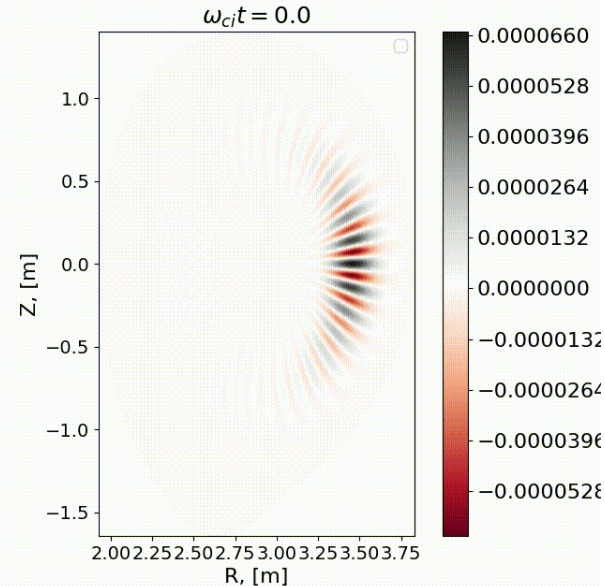
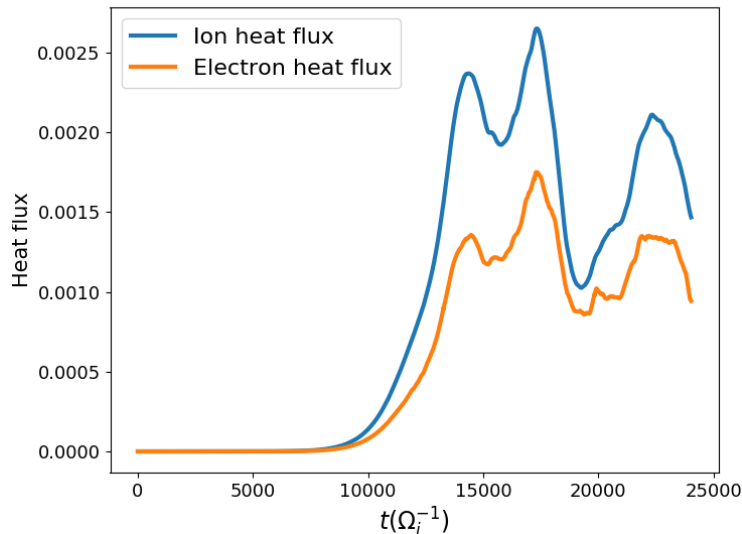
TAE and EPM instabilities in JET; frequency for n=5 TAE similar to LIGKA



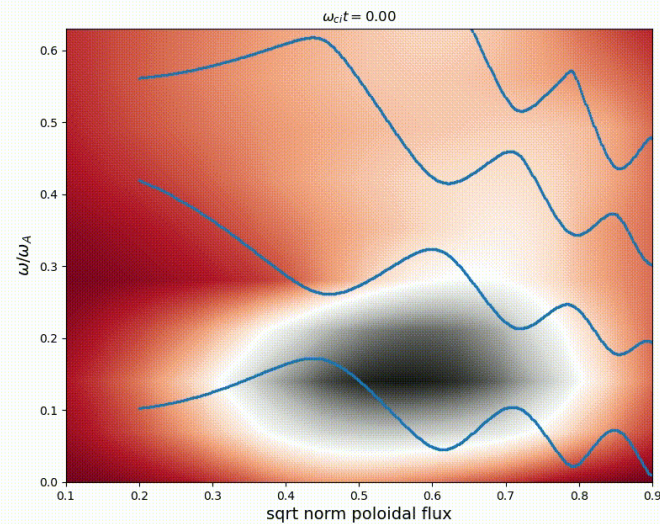
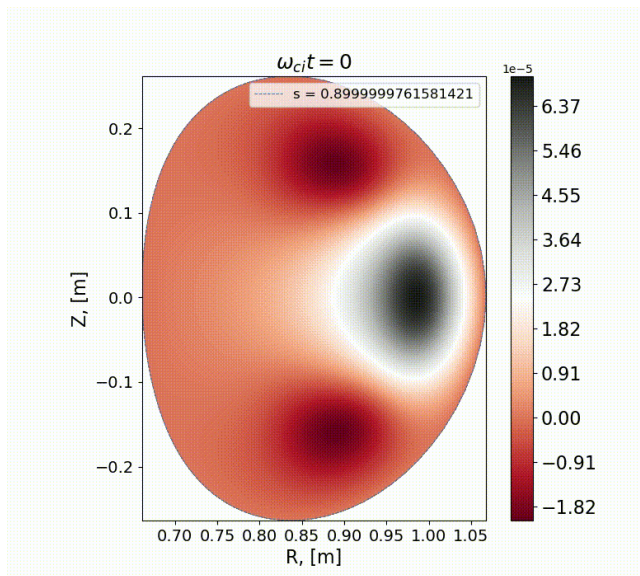
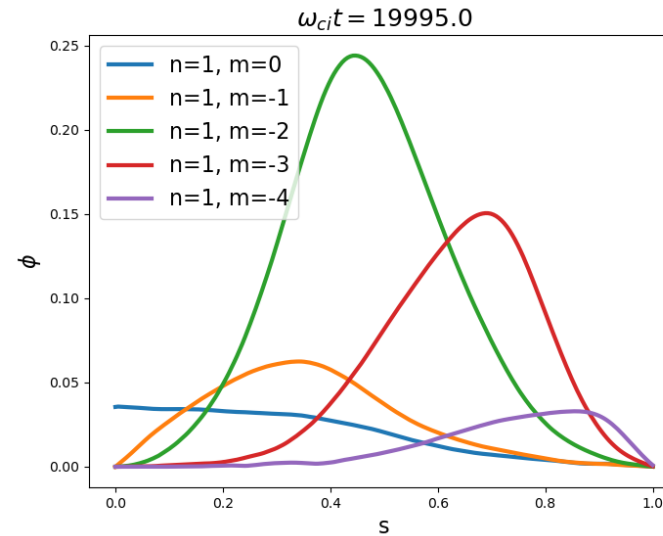
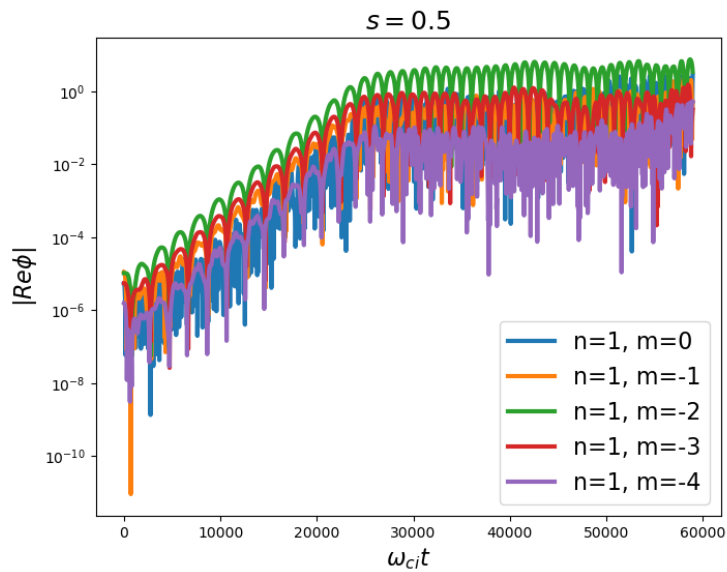
TAE/EPM instabilities in JET and turbulence



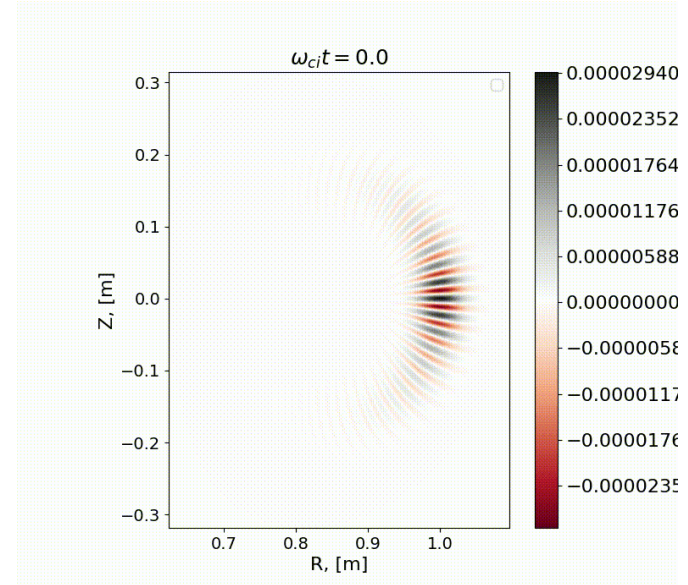
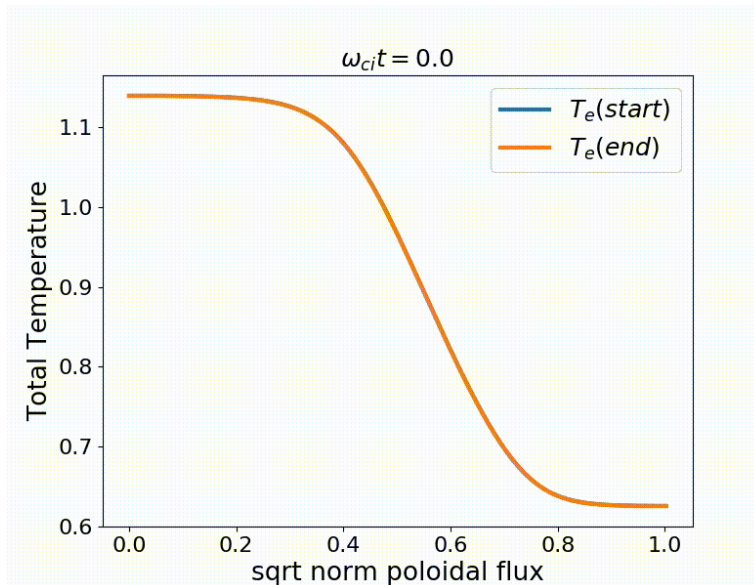
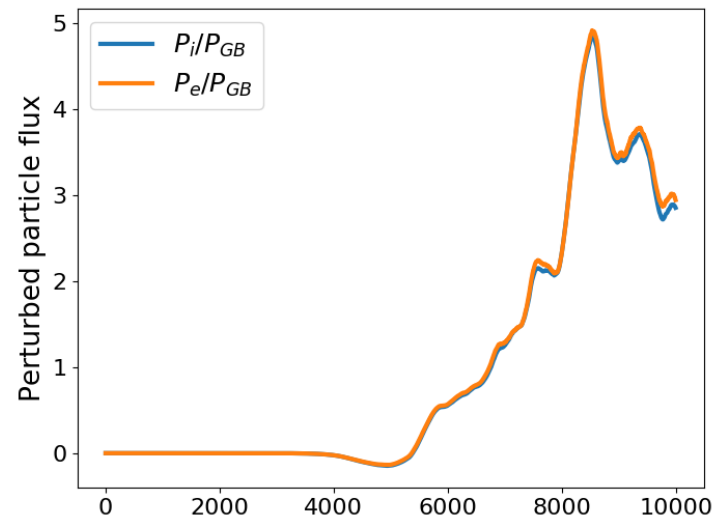
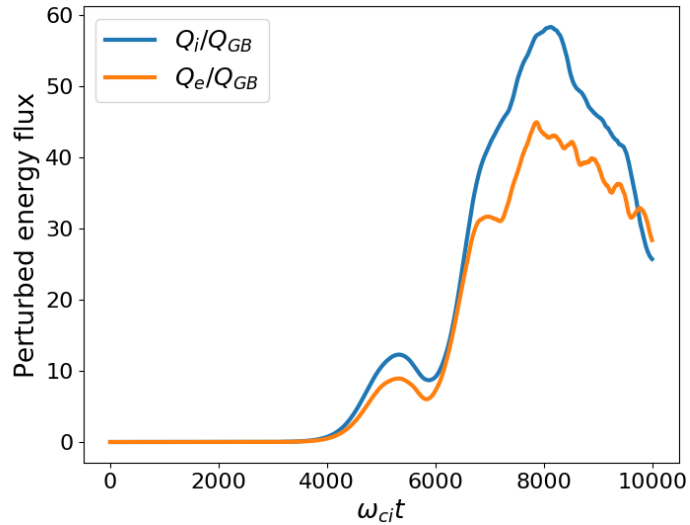
Mode structure: $n = 4, n = 5, n = 6$



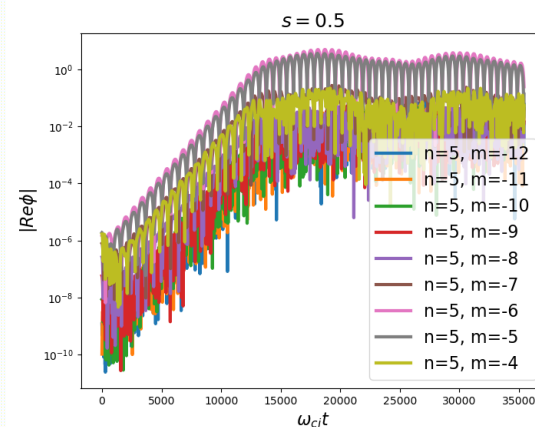
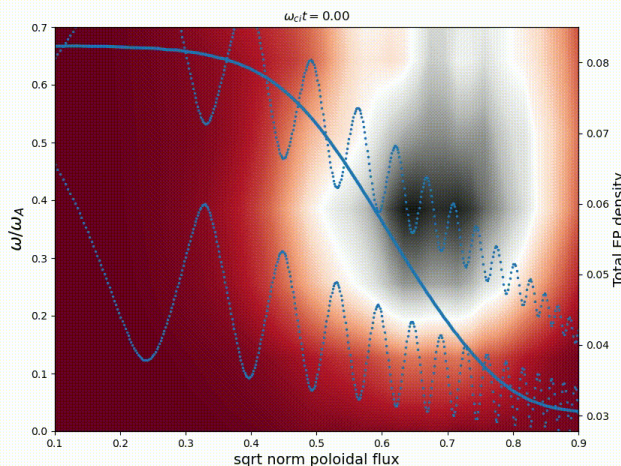
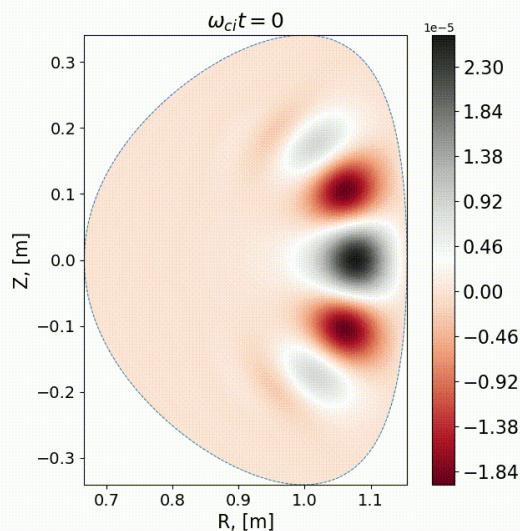
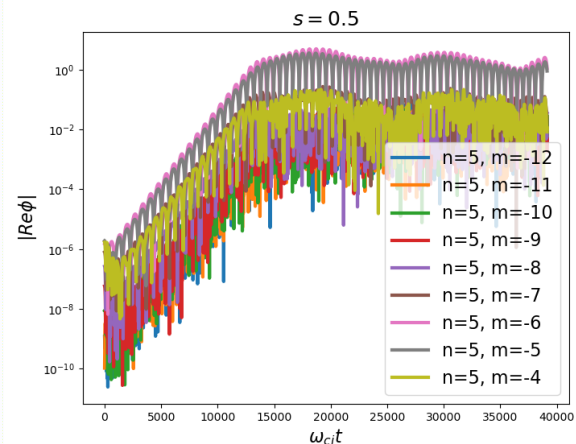
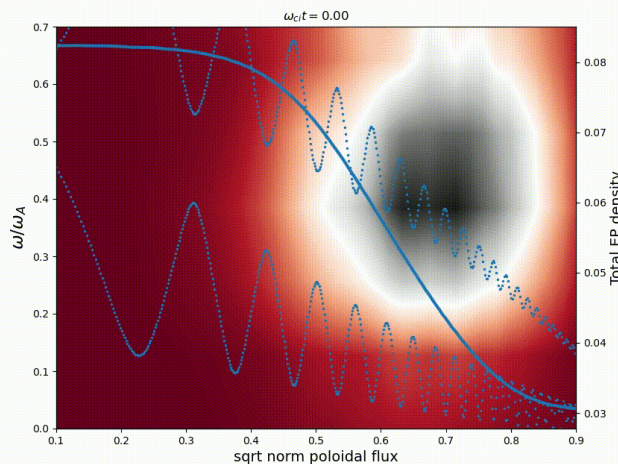
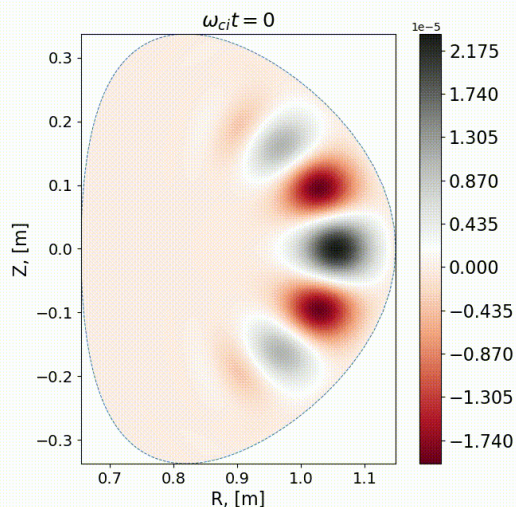
Chirping TAE/EPM instabilities in TCV



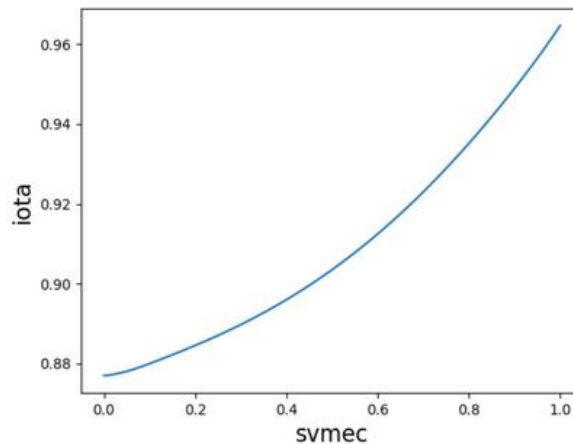
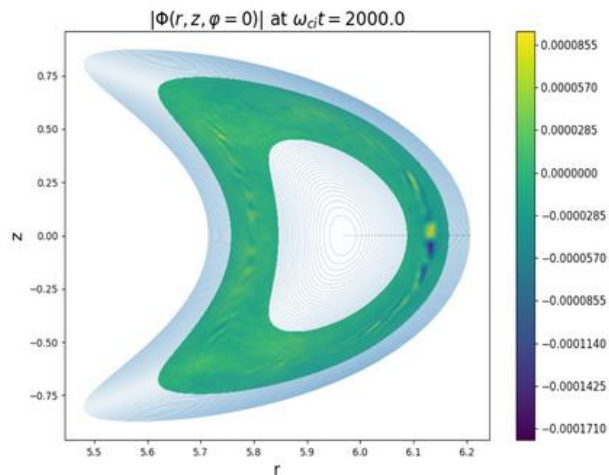
Electromagnetic turbulence in TCV



TAE/EPM: negative/positive triangularity TCV

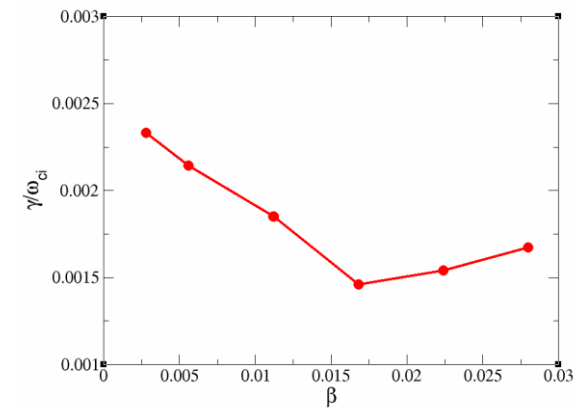
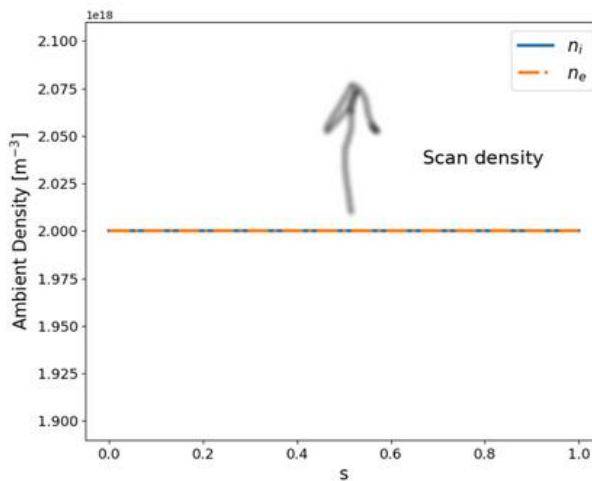
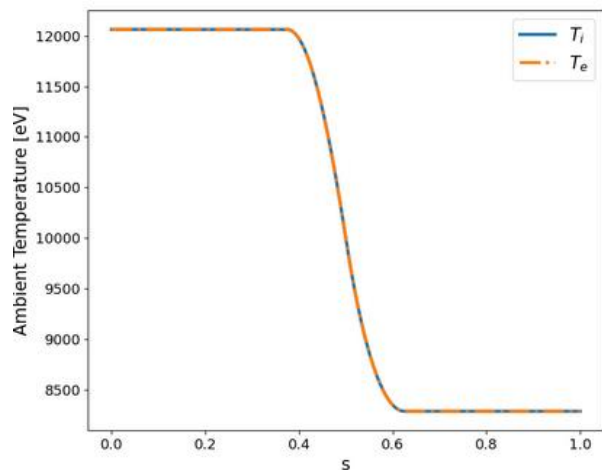


EM simulations in stellarators

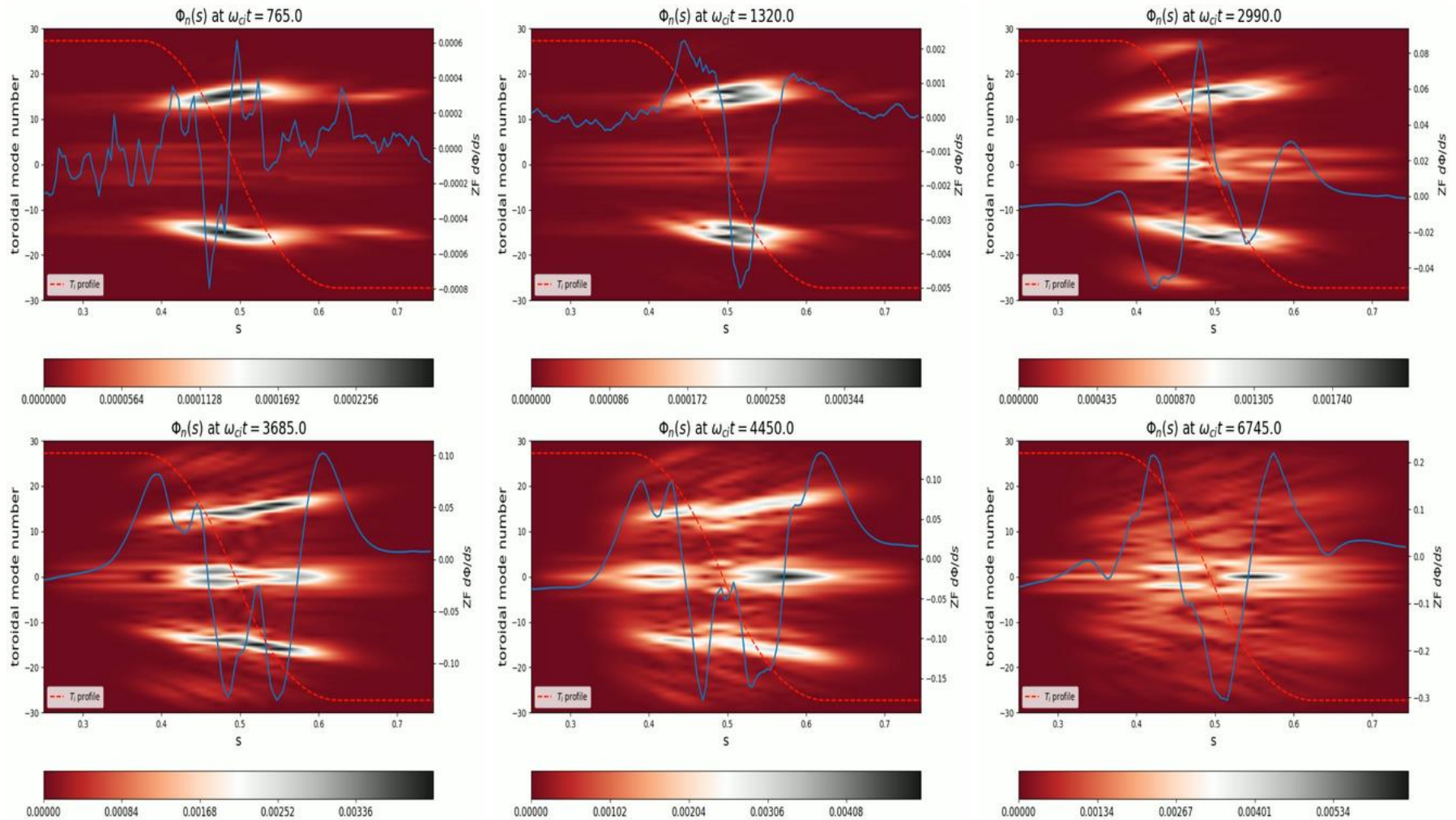


Larger temperature implies larger ρ_*

Larger ρ_* need less Fourier harmonics (to resolve the same $k \rho_i \sim 1$)



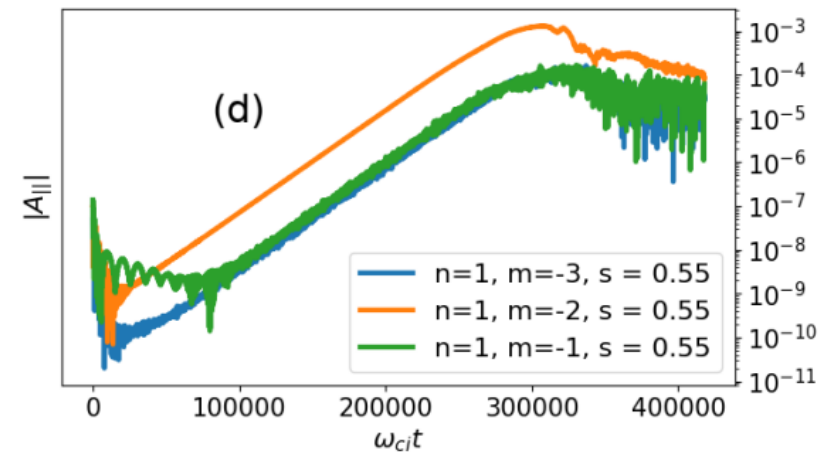
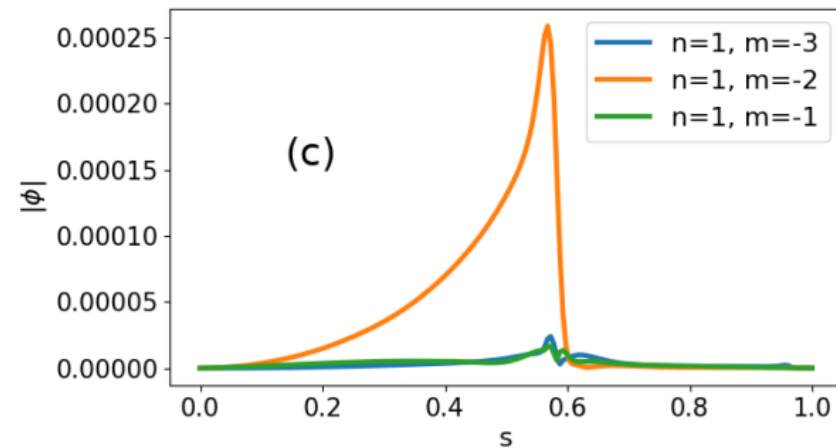
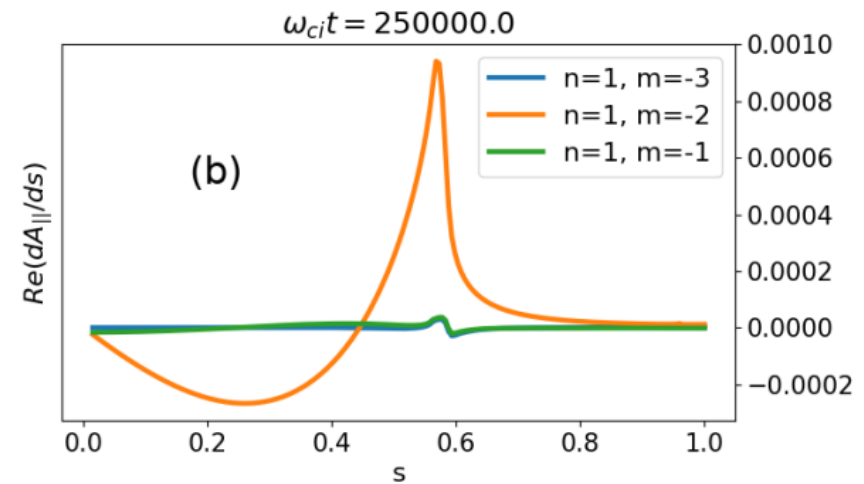
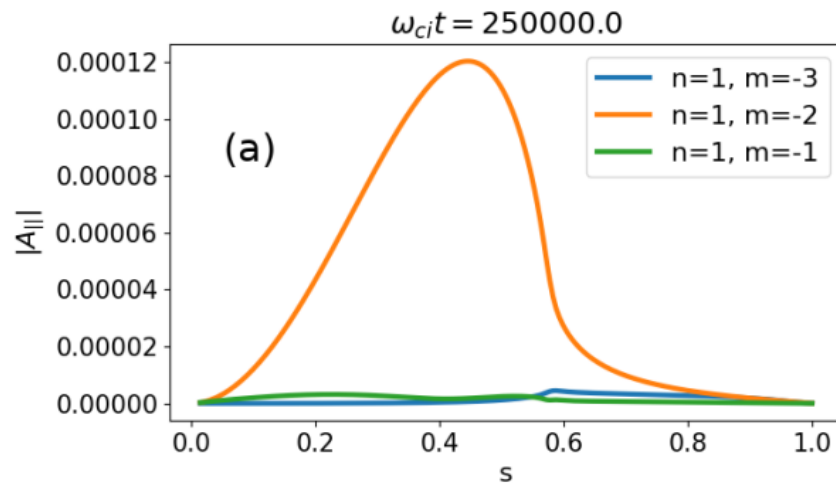
Toroidal spectrum: ZF and KBMs



Toroidal spectrum and zonal flow evolution for $\beta = 2.8\%$

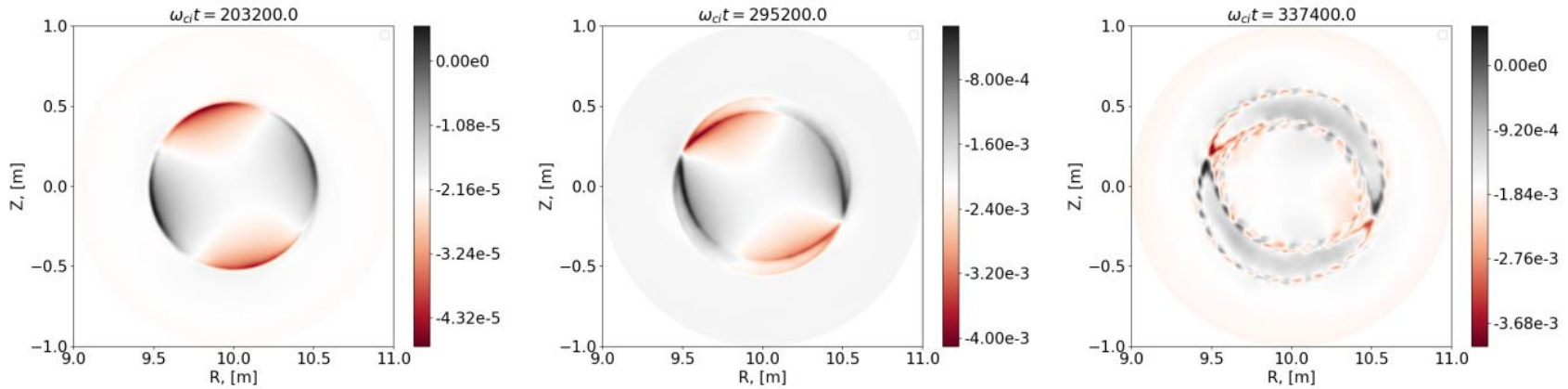
Zonal electric field (blue line) is driven self-consistently by stellarator turbulence

Tearing mode simulations

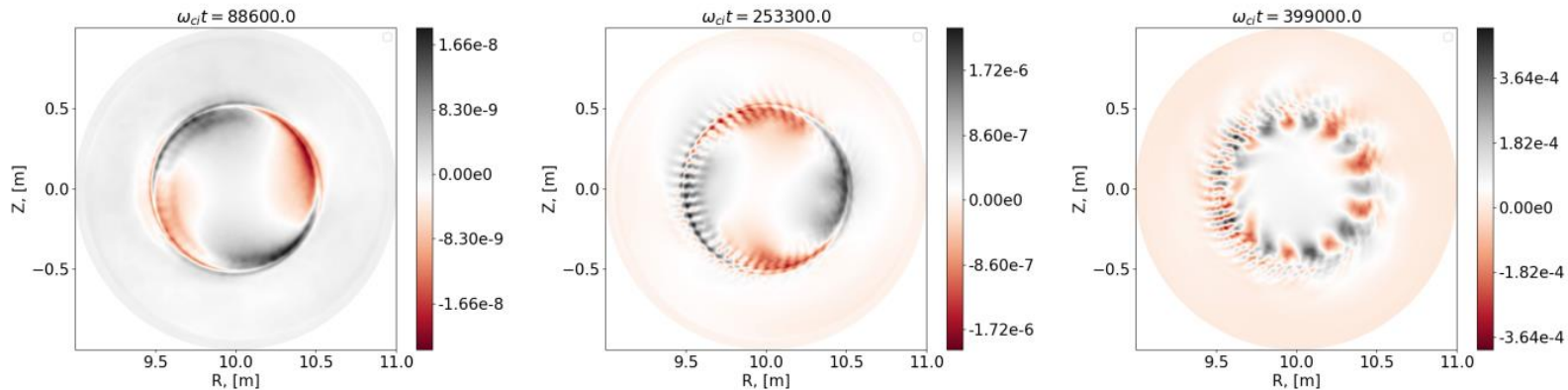


Safety factor profile with $q=2$ resonance; shifted Maxwellian for electrons
Tearing instability develops; peaked structures at resonant flux surface

Tearing mode simulations

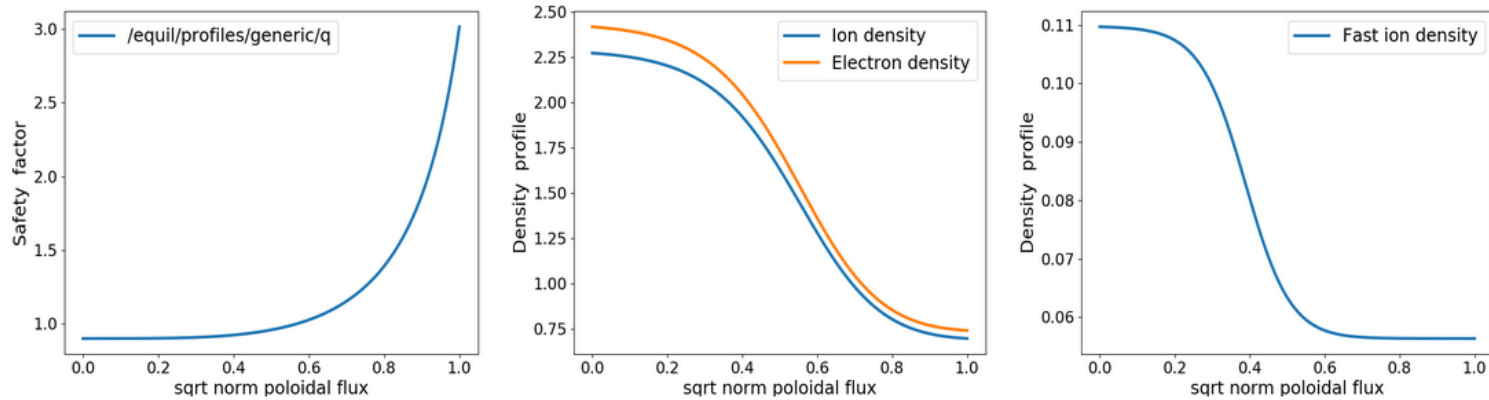


An island growth (X-points can be clearly seen); flat plasma profiles

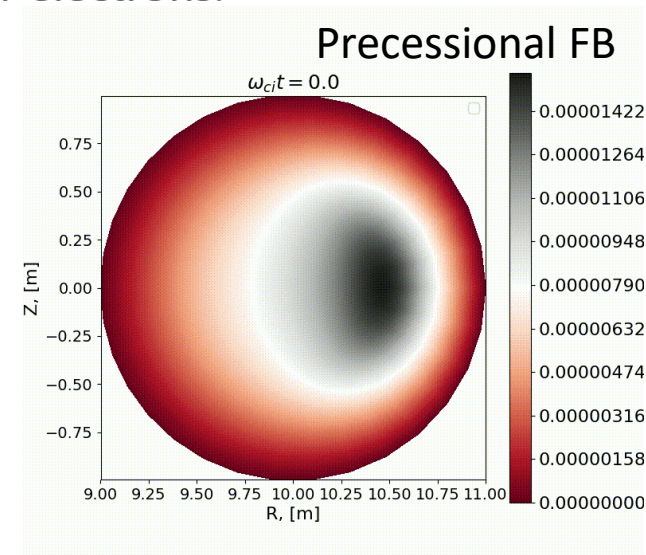
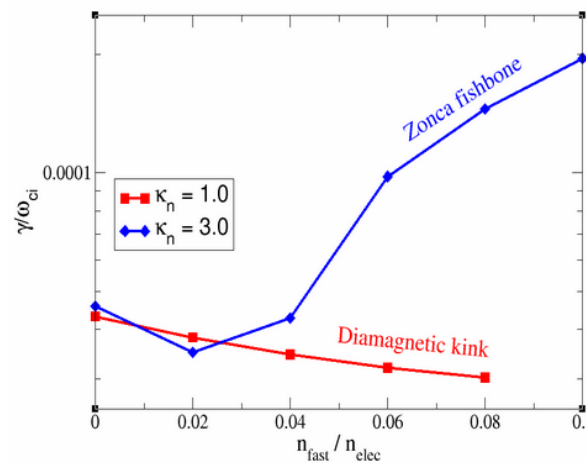
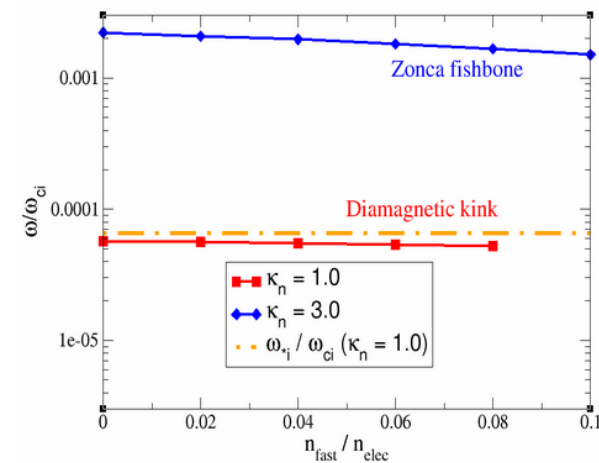


More complex physics for plasma with non-flat profile (turbulence)
It includes tearing, AEs, EM turbulence, and ZFs

Internal kink and fishbone instabilities



Large-aspect-ratio tokamak ($A=10$) with circular cross-sections. Safety factor ($q=1$ at $s=0.57$). Finite gradients for bulk-plasma density and EP density. Temperatures are flat for all species. Maxwellian fast ions; shifted Maxwellian for electrons.



Chirping TAEs



Electromagnetic turbulence and global modes

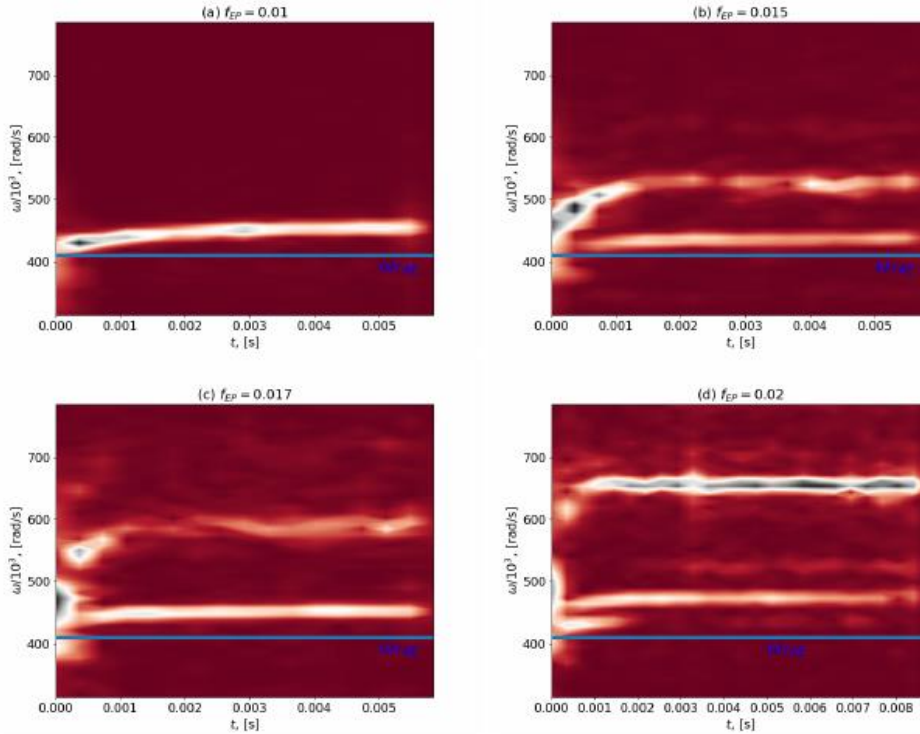
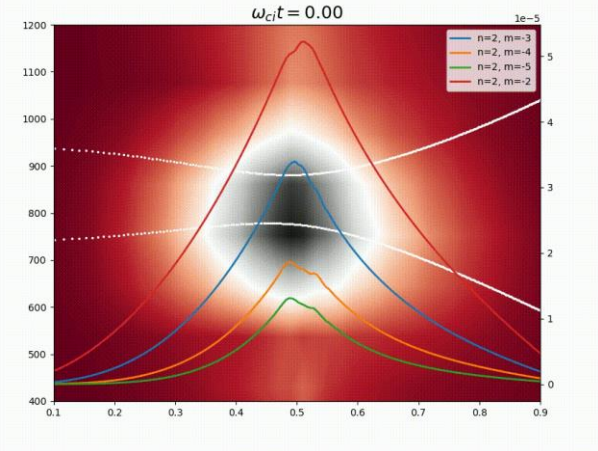
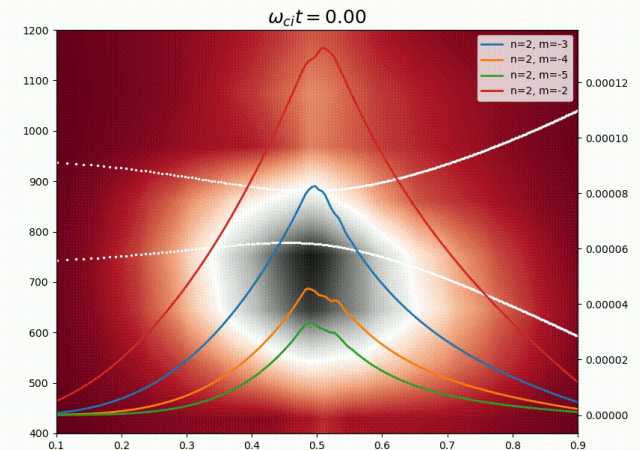


Figure 13. Energetic-particle nonlinearity only (flat bulk-plasma profiles). Frequency as a function of time for the fast-particle fraction: (a) $f_{EP} = 0.01$, (b) $f_{EP} = 0.015$, (c) $f_{EP} = 0.017$, (d) $f_{EP} = 0.02$. One sees how the nonlinear frequency evolution increases with the number of the fast particles.

9



No turbulence: mode stays at the TAE gap



In presence of turbulence (bulk-plasma dT/dr): frequency changes along continuum branch

Conclusions



- The creation and control of burning plasmas is an ultimate goal of magnetic fusion worldwide efforts. Tokamak and stellarator geometries are considered.
- One of the characteristic features of such plasmas is the intrinsic richness of their physics featuring complex couplings and interactions of microscopic turbulence with macroscopic MHD and Alfvén modes.
- In burning plasmas, such couplings may become especially strong since fast particles are abundant and can drive the macroscopic modes unstable.
- A global approach is needed to assess the physics combining the macroscopic modes, fast ions, Alfvénic instabilities, zonal flows, and turbulence.
- The global gyrokinetic particle-in-cell codes ORB5 and EUTERPE have been used to simulate the electromagnetic turbulence in the toroidal geometries of axisymmetric tokamaks and the more general stellarators.
- The so-called ITG-KBM transition has been identified and the relaxation of the profiles has been observed in a circular cross-section tokamak plasma and in the ASDEX-Upgrade geometry. First results from ITER, JET, and TCV.
- The multiscale physics has been addressed, showing the coupling of electromagnetic turbulence to the collisionless tearing instability and Alfvén modes destabilized by fast ions (including JET and TCV).
- Electromagnetic turbulence has also been addressed in the stellarator Wendelstein 7-X geometry. Turbulence spreading and generation of low-mode-number components.
- It has been demonstrated that such simulations are possible using existing global gyrokinetic particle-in-cell codes on the HPC systems already available for EUROfusion.

